ADVANCES IN MANUFACTURING SCIENCE AND TECHNOLOGY
Vol. 40, No. 2, 2016
DOI: 10.2478/amst-2016-0011

ADHESION INVESTIGATION OF RHODIUM ELECTROPLATED LAYERS ON NICKEL SUBSTRATE

Maryana Zagula-Yavorska, Krzysztof Krupa, Jan Sieniawski

Summary

The paper presents the evaluation of the quality and adherence of rhodium layers deposited on the nickel substrate. Rhodium layers (0.2 and 0.5 μm thick) were deposited by the electroplating method on the surface of the nickel substrate. The scratch test method (REVETEST R) was applied to determine the adhesion of layers. The increase of test force from 0.9 to 5 N and from 0.9 to 10 N did not lead to the rhodium layers detachment. Some microcracks were observed in the nickel substrate. The increase of load from 0.9 to 10 N leads to nested cohesive microcracks formation in the nickel substrate. Microcracks formed in the tensile stress field as a result of moving of the stylus. Good adherence of rhodium layers to the nickel substrate was observed.

Keywords: adhesion, layers, nickel, rhodium

Badania przyczepności powłok rodu do podłoża niklu

Streszczenie

Prowadzono analizę wyników badań przyczepności powłoki rodu do podłoża niklu. Powłoki rodu (o grubości 0,2 i 0,5 μm) wytwarzano metodą elektrochemiczną. Przyczepność tych powłok określono metodą zarysowywania. Stwierdzono, że liniowa zmiana wartości siły dociskającej wgłębnik od 0,9 do 5 N oraz od 0,9 do 10 N nie powoduje oderwania powłoki od podłoża. Zwiększenie obciążenia siły dociskającej wgłębnik od 0,9 do 10 N prowadzi natomiast do powstawania mikropęknięć w podłożu niklu.

Słowa kluczowe: przyczepność, powłoki, podłoże niklu, warstwa rodu

1. Introduction

Turbine blades made of nickel superalloys are crucial elements of the turbine and are subject to intensive destruction which is the result of variable stresses, high temperature and corrosion gases environment. The improvement of the engine efficiency by the increase of turbine inlet temperature implicates the use of different types of protecting coatings. The idea to apply a layer with protective properties on the surface of Ni-based superalloys was first practiced in the

Address: Prof. Jan SIENIAWSKI, Maryana ZAGULA-YAVORSKA, PhD Eng., Krzysztof KRUPA, PhD Eng., Rzeszow University of Technology, Department of Materials Science, 2 W. Pola St., 35-959 Rzeszów, e-mail: yavorska@prz.edu.pl

1960s [1]. Two types of protective coatings have been most widely used: diffusion aluminide coatings based on the β-NiAl phase and MCrAlY (M = Ni, Co, or NiCo) overlay coatings based on a mixture of β-NiAl and γ'-Ni_3Al or γ phases [1]. Addition of small amounts of reactive elements such as Zr, Hf, Y or Ce to the β-NiAl coating has beneficial effects on the oxidation behavior [2-3]. Reactive elements, such as hafnium and zirconium improve Al_2O_3 and Cr_2O_3 oxides adhesion and decrease their spallation. Zirconium and hafnium may be inserted to the coating in two ways: as alloying elements of the substrate or co-deposited with the coating. During oxidation hafnium diffuses from the substrate to the oxides layer and HfO_2 is being formed. HfO_2 oxides are places of heterogenic nucleation between CrO_2 oxides and delay CrO_2 oxides growth, while zirconium diffuses from the substrate to the oxides layer and delays pores formation at the Al_2O_3 – NiAl border and slows down oxides spallation [4-8]. High price and difficulties with hafnium and zirconium introduction to aluminides layers caused intensive research on introduction of other elements to improve corrosion and oxidation resistance of coated superalloys.

In this study rhodium layers (0.2 and 0.5 μm thick) were deposited on commercial nickel of 99.95% wt purity by the electroplating method. Adhesion of thin layers is an important issue for the assessment of the quality of coatings deposition. Adhesion strength of a layer-substrate system depends on the complex interaction of the test parameters (stylus properties and geometry, loading rate, displacement rate) and the layer/substrate properties (hardness, fracture strength, modulus of plasticity, damage mechanisms, microstructure, surface roughness). The scratch adhesion test can be performed one of two test modes – constant load and progressive load. In the constant load mode the normal force on the stylus is maintained at a constant level as the stylus moves at a constant displacement rate in relation to the test specimen surface. In the progressive load scratch test, the normal stylus force is linearly increased as the stylus moves at the constant displacement rate with respect to the test specimen surface [9]. The specific levels and types of damage in the scratch track are assessed with applied normal stylus forces. The normal force which produces a damage is defined as a critical scratch load (L_c). For a constant load test, the critical scratch load is defined by the constant normal force used in that particular scratch test. For a progressive load test, the critical scratch load is calculated by correlating the location of the defined damage with the normal stylus force [9]:

$$L_{CN} = [L_{rate} \cdot (l_n / x_{rate})] + L_{start} \tag{1}$$

where: L_{CN} – the critical scratch load for a defined type of damage, N; L_{rate} – rate of force application, N/min; l_n – the distance between the start of the scratch track and the start point of the defined type of damage in the scratch track, mm; x_{rate} –

the rate of horizontal displacement in the scratch test, mm/min; L_{start} – preload stylus force established at the start of the scratch test, N.

As different coatings have different modes of damage and failure, there is no universal damage mode. Bull [10] described general failure mechanisms for four combination of coatings and substrates (Tab. 1).

Table 1. Failure mechanisms in different substrate-coating combination, based on [10]

	Brittle substrate	**Ductile substrate**
Brittle coating	Tensile cracking in the coating followed by spalling and chipping of both the coating and the substrate	Tensile and Hertzian cracks in the coating progressing to chipping and spallation of the coating as the substrate is deformed
Ductile coating	Coating plastic deformation and conformal cracking, followed by spalling and buckling failure in the coating as the substrate cracks	Combined plastic deformation of the coating and the substrate producing tensile and conformal cracking with predominant buckling failure of the coating

Cracking, delamination, spalling and buckling can produce high frequency elastic waves in the coating and the substrate which can be detected by an acoustic emission system. As the applied normal force increases in the scratch test, coating damage events occur with increasing frequency and severity and the resulting elastic waves are detected, measured and recorded by the acoustic emission equipment. The acoustic emission data record for each scratch test are analyzed for significant changes in AE signal characteristics (peak amplitude, frequency, event counts, risetime, signal duration and energy intensity) that correlate with the given normal stylus force.

Bull and Blau [11] classified and described the different damage features obtained during the scratch test (Tab. 2).

It was presented common crack damage features (Fig. 1).

The purpose of this paper is to evaluate the quality of rhodium layers deposited on nickel substrate. To evaluate the quality of rhodium layers deposition adhesion test using the scratch test on the CMS Revetest device was performed.

2. Experimental procedure

Adhesion properties were evaluated using a CSM Revetest scratch tester. A scheme of the scratch test is presented in Fig. 2. The scratch is developed by drawing a diamond stylus of defined geometry and tip size (Rockwell C, 200 μm radius) across the flat surface of the specimen at a constant speed and progressively increasing normal force. The damage along the scratch track is determined by the acoustic emission by the optical microscope. The quantitative

scratch adhesion test system consists of six equipment subsystems: 1 – stylus and stylus mounting, 2 – mechanical stage and displacement control, 3 – test frame and force application system, 4 – force sensors, 5 – optical measurement and 6 – data acquisition/recording (Fig. 3).

Table 2. Categories, terms and description of crack damage features, based on [10, 11]

Category	Damage term	Description
1. Through-thickness cracking and cohesive failure	Brittle tensile cracking	Series of nested micro-cracks, some of which are semicircular, arcs open toward the direction of scratching and formed behind the stylus.
	Hertz cracking	Series of nested, nearly-circular micro-cracks within the scratch groove.
	Conformal cracking	Cracking due to the coating trying to conform to the shape of the scratch groove. Less sharp than tensile or hertz cracks; arcs open away from the direction of scratching.
2. Spallation and adhesive failure	Buckling	Coating buckles ahead of the tip, producing irregularly-spaced arcs opening away from the direction of scratching. Common for thinner coatings.
	Buckle spallation	Similar to buckling, but with wide, arc-shaped patches missing.
	Wedging spallation	Regularly-spaced and shaped, annular circular that extend beyond the edges of the groove, caused by a delaminated region wedging ahead to separate the coating. Commonly seen in thicker coatings.
	Recovery spallation	Regions of detached coating along one or both sides of the groove. Produced by elastic recovery behind the stylus and depends on plastic deformation in the substrate and cohesive cracking in the coating.
	Gross spallation	Large sections of detached coating within and extending beyond the groove. Common in coatings with low adhesion strength or high residual stresses.
3. Chipping		Rounded regions of coating removal extending laterally from the edges of the groove.

Deposition of rhodium layers (0. 2 and 0.5 μm thick) on the nickel substrate was performed by the electroplating method. Before rhodium layers deposition, the substrate was grounded by abrasive up to SiC No 1000, degreased in ethanol and ultrasonically cleaned. For the 3 mm scratch length, the applied load was progressively increased from 0.9 N to 5 N at a rate 8.2 N/min and from 0.9 to 10 N at a rate 18. 2 N/min. Acoustic Emission signals were recorded during the test by the sensor attached to the load arm. Five measurements were performed at the room temperature for each sample. Nanoindentation testing was carried out

using the CSM nanohardness tester. The hardness and Young's modulus were determined by the Oliver and Pharr method [12]. The surface roughness parameter – *Ra* was evaluated by the S2 MAHR Perthometer.

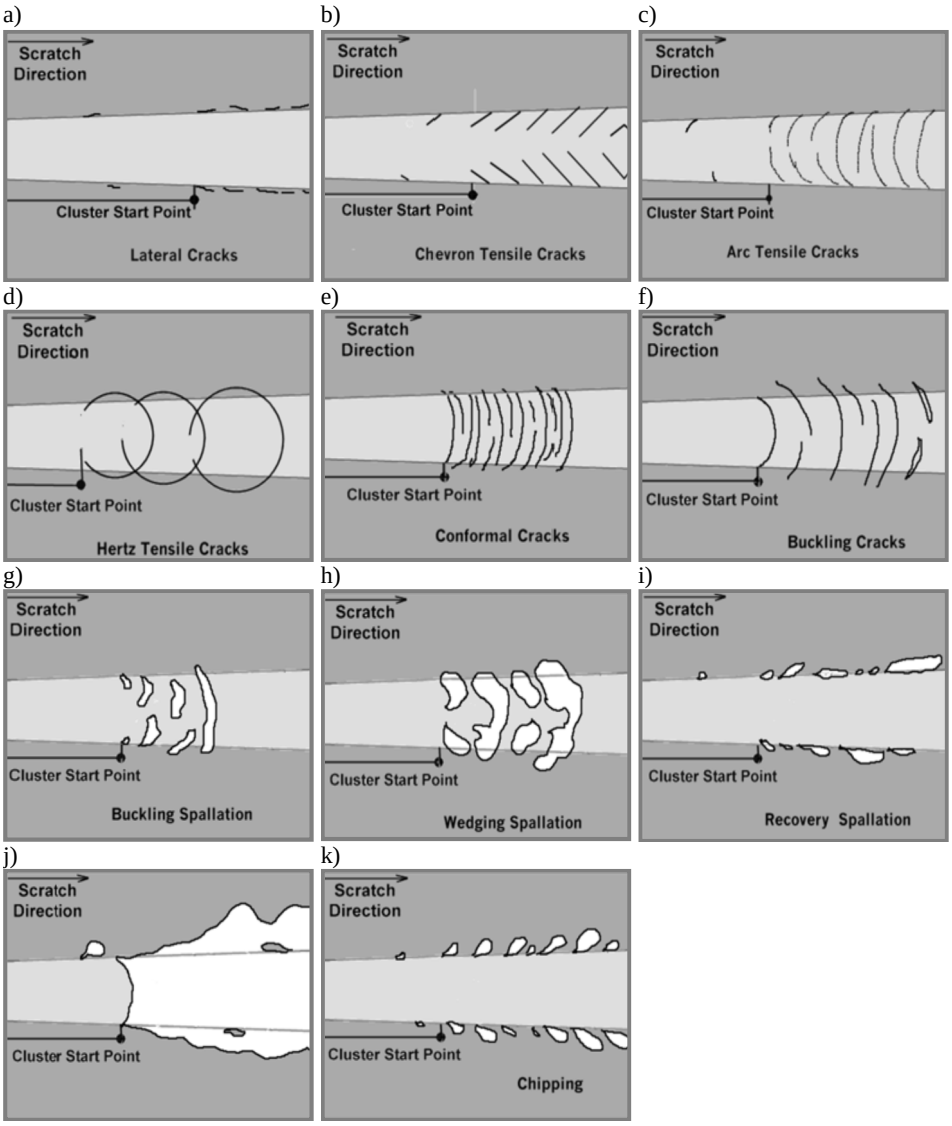

Fig. 1. A scheme and kinds of crack damage: a) lateral cracks; b) forward chevron tensile cracks; c) arc tensile cracks; d) hertz tensile cracks; e) conformal cracks; f) buckling cracks; g) buckling spallation; h) wedging spallation; i) recovery spallation; g) cross spallation; k) chipping, based on [9-11]

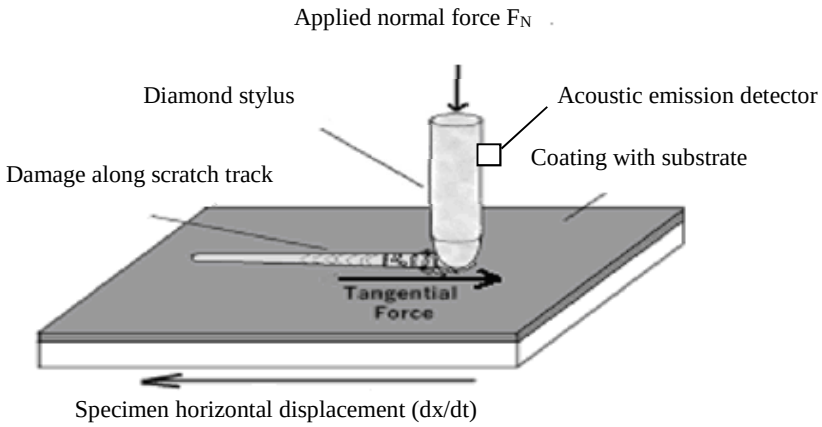

Fig. 2. A scheme of scratch test

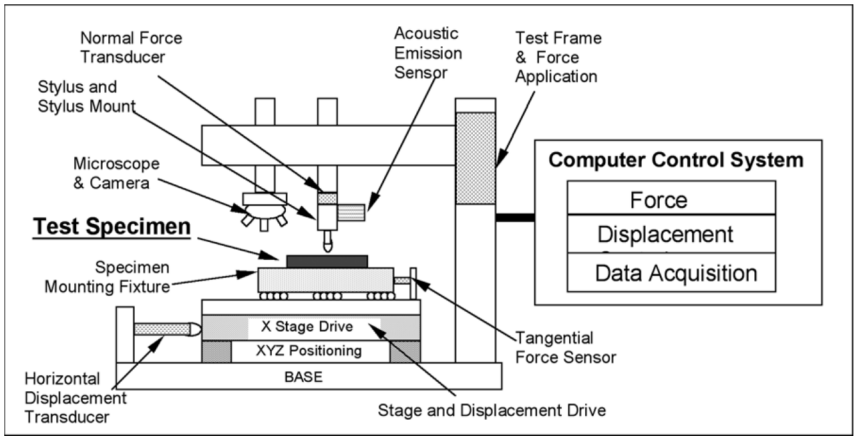

Fig. 3. Schematic of computerized REVETEST for control and storage results, based on [9]

3. Results and discussion

The adhesion strength is a complicated function of interface conditions, such as layers thickness, surface roughness and elastic properties of the substrate [13]. Therefore, roughness of the nickel substrate before and after rhodium electroplating was measured. It was found that rhodium electroplating process leads to decrease of the surface roughness parameter *Ra* (Table 3). Hardness of the nickel substrate is about 190 HV0.1 whereas Young's modulus of the substrate is about 169 GPa. The hardness of the rhodium layer is 8.5 GPa and the associated Young's modulus is 301 GPa [13].

Table 3. Values of the surface roughness parameter *Ra* before and after rhodium electroplating, hardness and Young's modulus of the nickel substrate

Substrate	Roughness *Ra*, µm			HV0.1	Young's modulus (GPa)
	Without the layer	Rhodium electroplating layer thickness			
		0.2 µm	0.5 µm		
Nickel	0.150	0.09	0.08	190	168

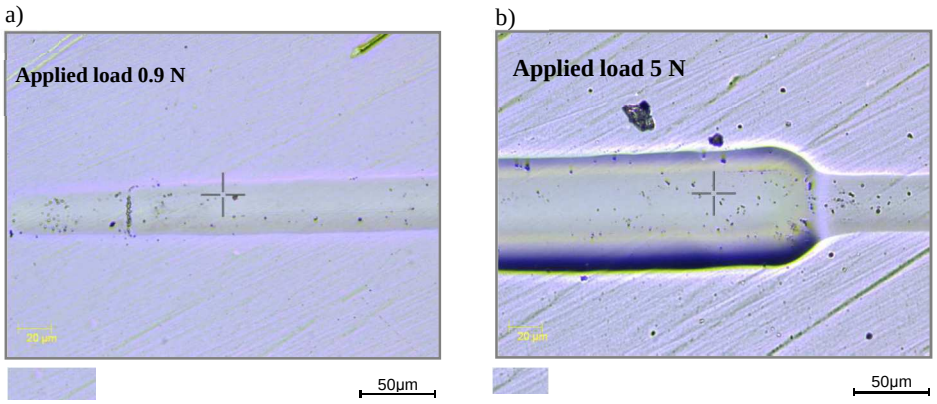

Fig. 4.Scratch track of rhodium layer (0.2 µm thick) deposited on pure nickel: a) the beginning of the scratch track; b) the end of the scratch track

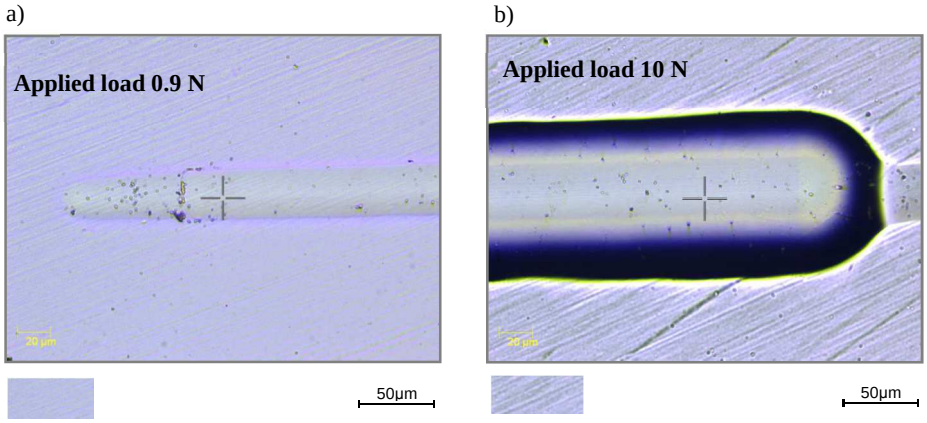

Fig. 5. Scratch track of rhodium layer (0.2 µm thick) deposited on pure nickel: a) the beginning of the scratch track; b) the end of the scratch track

The scratch track of rhodium layer (0.2 µm thick) at the beginning of the process and at the end of the process using progressive load from 0.9 to 5 N is presented in Fig. 4a,b. The damage of rhodium layer was not observed. The

increase of the progressive load from 0.9 to 10 N did not damage the rhodium layer and no microcracks occurred both at the early stage and final stages of the scratch test (Fig. 5a, b).

Increase of the rhodium thickness from 0.2 to 0.5 μm does not lead to detach of the rhodium layer from the substrate (Fig. 6 a, b). The use of the progressive load from 0.9 to 10 N resulted in the first microcracks appearance (Fig. 7 b). The lack of acoustic emission signals confirms the good adhesion of the rhodium layer (0.2 and 0.5 μm thick) to the nickel substrate (Figs. 8 a, b). It was observed that, the thin layer depressed under the stylus that resulted in the stylus penetration on the higher depth in comparison to the thick layer (Fig 9 a, b).

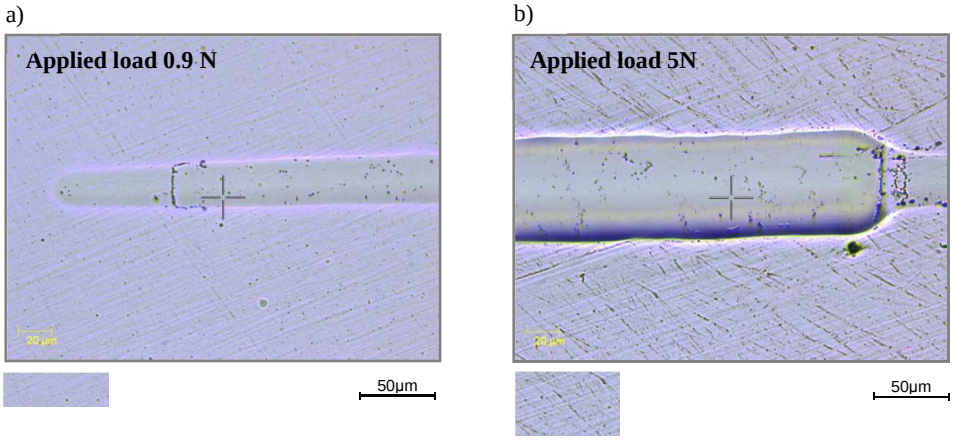

Fig. 6. Scratch track of rhodium layer (0.5 μm thick) deposited on pure nickel: a) the beginning of the scratch track; b) the end of the scratch track

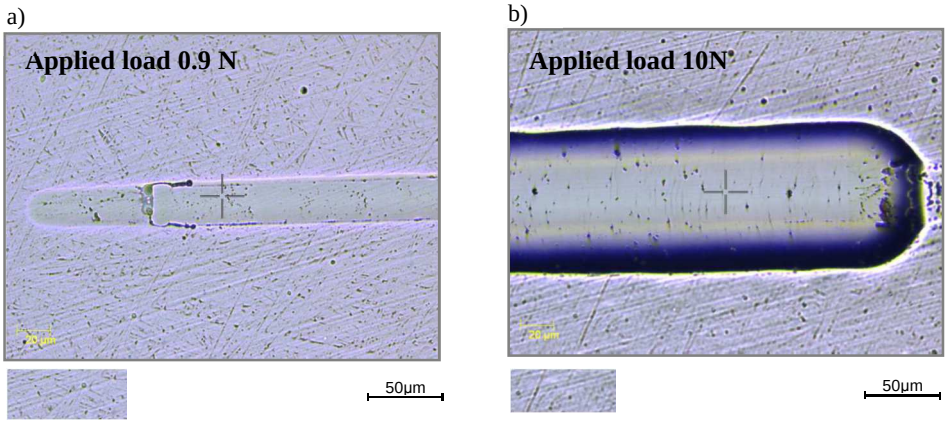

Fig. 7. Scratch track of rhodium layer (0.5 μm thick) deposited on pure nickel: a) the beginning of the scratch track; b) the end of the scratch track

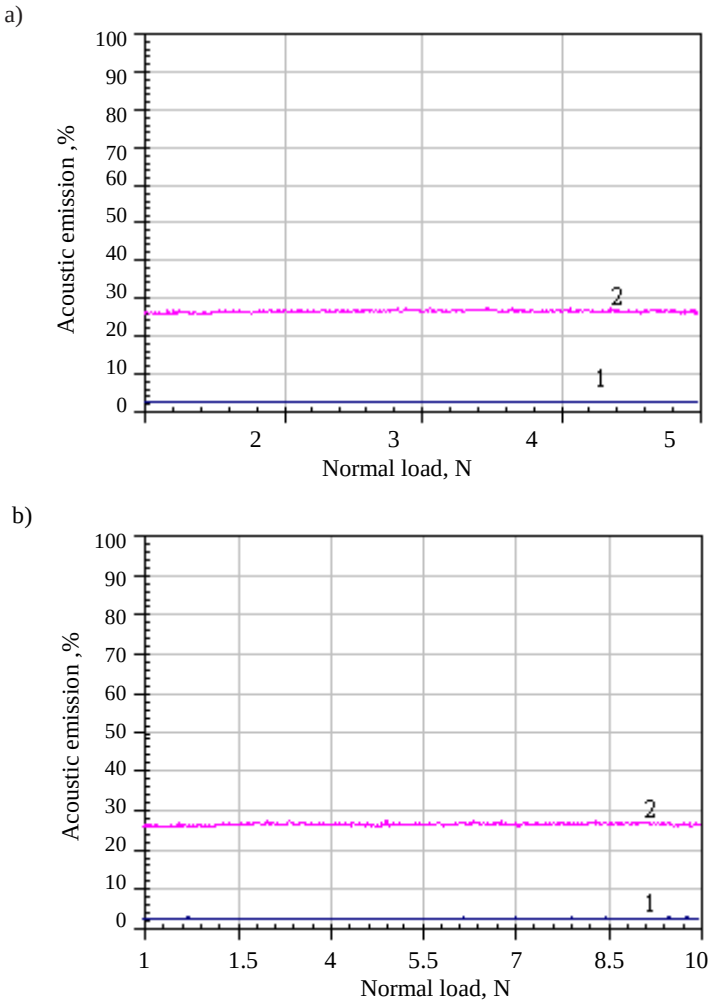

Fig. 8. Acoustic emission during a scratch measurement of 1 – 0.2 μm thick rhodium and 2 – 0.5 μm thick rhodium deposited on pure nickel: a) progressive load from 0.9 to 5 N; b) progressive load from 0.9 to 10 N

The series of nested cohesive semicircular microcracks form in the tensile stress field in the wake of the moving stylus [14]. The lack of acoustic emission signals is associated with the ductile failure. Whereas, the increase of the coated substarte (0.5 μm rhodium thick) load from 0.9 to 10 N leads to the increase of the energy of elasto-plastic waves and causes the tensile stress formation in the nickel substrate. This phenomena leads to the microkracks formation in the nickel substrate. Nevertheless, rhodium layers (0.2 and 0.5 μm thick) have good adherence to the nickel substrate.

a)

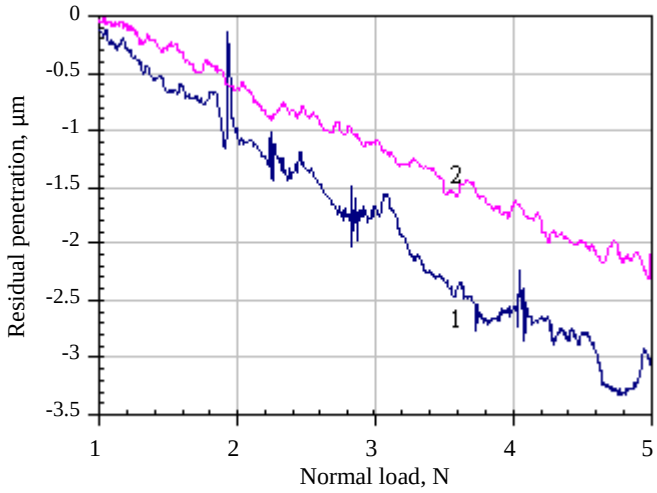

b)

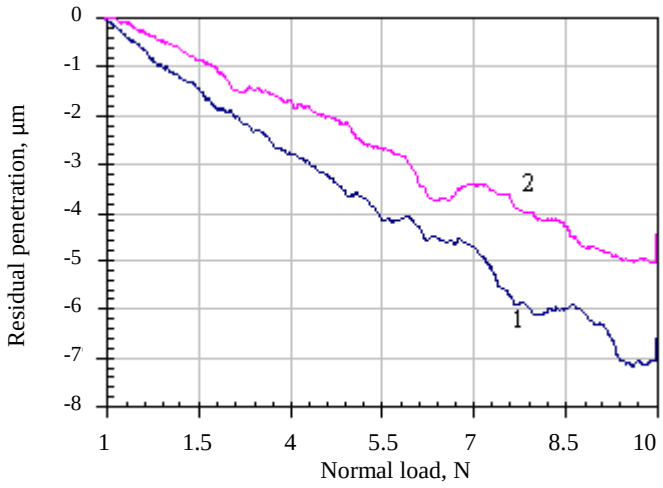

Fig. 9. Residual penetration during a scratch measurement of 1 – 0. 2 µm thick rhodium and 2 – 0.5 µm thick rhodium deposited on pure nickel: a) progressive load from 0.9 to 5 N; b) progressive load from 0.9 to 10 N

4. Conclusions

It was found, that rhodium layers (0.2 and 0.5 µm thick) deposited on pure nickel have good adherence to the substrate. The lack of damage of rhodium layers and no microcracks were observed in the rhodium layer (0.2 µm thick) during the applied progressive load both from 0.9 to 5 N and from 0.9 to 10 N. Some

microcracks were identified in the rhodium coated (0.5 µm rhodium thick) nickel substrate at the 10 N load and on the depth of 5 µm from the scratch surface. Such large load caused the tensile stresses generating and microcracks formation in the nickel substrate.

The present study shows, that from the point of view of adhesion properties, nickel is a good choice as a substrate material for rhodium layers deposition. Therefore it seems that further research on rhodium modified aluminide coatings should be carried on.

References

[1] N. LEE: Current status of environmental barrier coatings for Si-based ceramics. *Surface and Coatings Technology*, **133-134**(2000), 1-7.
[2] J. ROMANOWSKA, M. ZAGULA-YAVORSKA, J SIENIAWSKI: The zirconium influence on the microstructure of the aluminide coatings deposited on the nickel substrate by the CVD method. *Bulletin of Materials Science*, **36**(2014), 1043-1048.
[3] J. ROMANOWSKA et al.: Zirconium modified aluminide coatings obtained by the CVD and PVD methods. *Open Journal of Metal*, **3**(2013), 92-99.
[4] M. ZIELIŃSKA et al.: Microstructure and oxidation resistance of an aluminide coating on the nickel based superalloy Mar M247 deposited by the CVD aluminizing process. *Archives of Metallurgy and Materials*, **3**(2013), 697-701.
[5] S. BOSE: High temperature coatings. Burlington 2007.
[6] Y. WANG, M. SUNESON, G. SAYRE: Synthesis of Hf-modified aluminide coatings on Ni-base superalloys. *Surface and Coatings Technology*, **206**(2011), 1218-1228.
[7] R. PRESCOT et al.: Oxidation mechanism of β-NiAl+Zr determined by SIMS. *Corrosion Science*, **37**(1995), 1341-1346.
[8] D. LI et al.: Cyclic oxidation of β-NiAl with various reactive element dopants at 1200 ºC. *Corrosion Science*, **66**(2013), 125-135.
[9] ASTM C1624-05 Standard test method for adhesion strength and mechanical failure modes of ceramic coatings by quantitative single point scratch testing.
[10] S. BULL: Can the scratch adhesion test ever be quantitative. Utrecht-Boston, Koln, 2001.
[11] P. BLAU: Handbook of scratch testing. Oak Ridge 2002.
[12] W. OLIVER, G. PHARR: An improved technique for determining hardness and elastic modulus using load and displacement sensing indentation experiments. *Journal of Materials Research*, **7**(1992), 1564-1578.
[13] L. MAROT et al.: Adhesion of rhodium films on metallic substrates. *Thin Solid Films*, **516**(2008), 7604-7608.
[14] J. KAMMINGA, P. ALKEMADE, G. JANSEEN: Scratch test analysis of coated and uncoated nitrided steel. *Surface and Coatings Technology*, **177/178**(2004), 284-288.

Received in February 2016